Single-molecule characterization of near-infrared-emitting silver nanoclusters

Hooley, Emma Nicole; Paolucci, Valentina; Liao, Zhiyu; Carro, Miguel; Vosch, Tom André Jos

Published in:
Advanced Optical Materials

DOI:
10.1002/adom.201500048

Publication date:
2015

Document version
Publisher's PDF, also known as Version of record

Single-Molecule Characterization of Near-Infrared-Emitting Silver Nanoclusters

*Emma N. Hooley, Valentina Paolucci, Zhiyu Liao, Miguel R. Carro Temboury, and Tom Vosch**

In this paper, single molecule spectroscopy is used to probe the photophysical heterogeneity of near-infrared emitting silver nanoclusters stabilized in single stranded DNA containing 24 cytosines (C24-AgNCs). Focusing on this subset of emitters allows us to address and correlate their photophysical parameters. The results suggest that for these near-infrared emitting C24-AgNCs, the broad range of observed photophysical properties is due to the spectral heterogeneity of two species, one of which has a broad range of emission maxima and decay times. This conclusion is drawn by analyzing the results of a large number of single C24-AgNCs where, for the first time, emission maxima, fluorescence decay times, fluorescence intensity, blinking, and photon antibunching are determined simultaneously. The single molecule measurements also reveal that some of the C24-AgNCs can change their spectral properties during the measurement, while photon antibunching measurements verified that all the analyzed C24-AgNCs behave as single emitters. While the overall spectral heterogeneity can be related to the immobilization in the polymer film and/or intrinsic heterogeneity of the C24-AgNCs emitters, the exact origin of the dynamical changes has not been fully determined. However, changes in the AgNCs geometry, local environment, or changes in the DNA conformation are possible explanations.

1. Introduction

Advances in biological imaging have led to an increased need for appropriate fluorophores for imaging. Besides classic organic dyes, fluorescent proteins and quantum dots, noble metal nanoclusters have emerged as a viable and exciting material for use in modern microscopy.[1–4] Some silver nanoclusters (AgNCs) have been reported to be bright and have high photostability in polymer films[5,6] and, as they consist of between ≈2 and 20 silver atoms,[7,8] are small enough to minimally impact the target molecule.[9] AgNCs exhibit fluorescence from well defined, molecule-like electronic energy levels.[10,11] They have the tendency to agglomerate[12] in solution, however, are readily stabilized by polymers,[13] dendrimers,[14] peptides or proteins,[9,15,16] and most commonly, single stranded DNA (ssDNA).[5,6,17] Cytosine rich ssDNA is commonly used to stabilize emissive AgNCs as silver ions have been shown to have a strong affinity for cytosine,[18,19] though the latter is not a necessity.[7,20] The small size and biocompatibility of the stabilizing molecule make these AgNCs particularly useful for biological imaging.[21] Clusters stabilized by short peptides can diffuse through cell membranes in live cells[15] and it has been shown that DNA AgNCs can bind to cell surfaces.[22]

A wide palette of silver nanoclusters has been reported, covering the spectrum from blue to NIR.[4,23] Of these, the NIR emitting clusters are the most sought after for biological imaging, as redshifted excitation and emission reduces the problem of autofluorescence. It has been suggested that the variety of emission colors is due to differences in the size, charge, and geometry of the clusters.[23–25] Small changes in the DNA sequence can also lead to significant changes in the observed emission.[17]

Precise control of silver nanocluster synthesis is difficult, as large biomolecules, like DNA, exist in a variety of conformations and states, many of which are closely dependent on the surrounding microenvironment. Careful synthesis, or clever manipulation of the DNA scaffold[26] can go some way to ensuring the population of nanoclusters is relatively homogeneous, although most studies rely on spectral selection to look at specific nanocluster populations. Separation of silver nanocluster species may also be achieved by high-performance liquid chromatography (HPLC).[7] While HPLC is useful for studying a single population of nanoclusters, it is time consuming and does not allow for separation of clusters with similar retention times. In order to probe the heterogeneity of AgNC populations, single molecule spectroscopy is a useful tool, as clusters are studied individually allowing for definitive separation and the construction of histograms of specific photophysical properties.[6,27,28]

Dr. E. N. Hooley, Z. Liao, M. R. Carro Temboury, Prof. T. Vosch
Nano-Science Center/Department of Chemistry
University of Copenhagen
Universitetsparken 5, 2100 Copenhagen, Denmark
E-mail: tom@chem.ku.dk

V. Paolucci
Dipartimento di Chimica, Biologia e Biotecnologie
Università Degli Studi di Perugia
Via Elce di Sotto, 8, 06123 Perugia, Italy

DOI: 10.1002/adom.201500048

In this paper we used a polycytosine single stranded DNA containing 24 cytosines to stabilize near-infrared emissive AgNCs (C24-AgNCs). Polycytosines can stabilize a whole range of emitters that cover the visible range, hence making it a good candidate to study the photophysical heterogeneity at the single molecule level. In this case, we focus on the near-infrared emitters using 633 nm as the excitation wavelength. Although a number of single molecule studies have been performed on AgNC to investigate specific photophysical parameters,[5,6,8,10,14,25,27–33] we simultaneously measure several photophysical properties for each individual cluster, including decay times, emission spectra, and antibunching. This allows us to compare and correlate these photophysical properties within a sample to better understand the photophysical behavior and heterogeneity of these complex as-synthesized AgNC samples.

2. Results and Discussion

2.1. Ensemble Measurements

A sample of AgNCs was prepared in Milli (MQ) water and the typical emission spectra upon excitation at 635 nm can be seen in Figure S2A (Supporting Information). The emission spectrum exhibits a maximum at 695 nm and a full width half maximum value of 100 nm. It is similar to the spectra of NIR emitters from AgNC-C24 published in refs. [21,22,34] as well as the spectra of AgNCs stabilized in other polycytosine sequences.[6] Time-correlated single photon counting (TC-SPC) experiments exciting at 635 nm and monitoring the emission at 692 nm were performed. The decay curve could be best fitted with a four exponential decay model. The fluorescence decay contains a large component of 3.09 ns with a fractional contribution of 82.8%, followed by a smaller 11.8% component which has a decay time of 5.26 ns. There are also two additional shorter decay components with minor contributions (see Table S1, Supporting Information, for details). These nanosecond decay time values are in line with results from other AgNCs spanning the entire visible range.[4] Monoexponential,[35] biexponential,[23] as well as more complex fits[36] have been used to describe the fluorescence decay curves of as-synthesized AgNCs, which points to complex, heterogeneous solutions containing more than one emitting species. In order to better understand the heterogeneity and number of emissive species that are present in the as-synthesized sample, we turn to single molecule spectroscopy.[37] For this, the C24-AgNC solution was diluted and mixed with a poly-vinyl alcohol (PVA) solution. Spincoating resulted in immobilized and spatially separated C24-AgNC (see Figure S1, Supporting Information, for an example).

2.2. Single Molecule Measurements: Decay Times

Figure 1b shows the fluorescence trajectory of a single C24-AgNC in PVA. The clusters are usually bright and photostable, with survival times in the order of tens to hundreds of seconds (see Figure S3A, Supporting Information) when using 108 W cm^{-2}, and high emission rates in the order of thousand to ten thousand counts per second (see Figure 3B, Supporting Information). The majority of C24-AgNC are photobleached within 250 s; however, several emitted photons for thousands of seconds before photobleaching. This is consistent with previous polycytosine samples that have shown good stability in PVA film.[6] Not all AgNCs have such excellent chemical and photostability, especially in solution.[20,38] The fluorescence decay times are calculated every 10 000 photons and plotted alongside the fluorescence trajectory (Figure 1a). Of the 289 C24-AgNCs measured, the overwhelming majority could be fitted with a monoexponential decay function (285 of 289, 99%). The remaining four C24-AgNCs had to be fitted with a biexponential decay, which had an additional short decay time component with a small contribution. These clusters were not included in further analysis. A histogram of fluorescence decay times, built using the average decay time from each C24-AgNC, is shown in Figure 1d. The decay time is averaged over the measurement time of each cluster, as the decay time sometimes changes during the measurement. Figure 1a shows the decay time jumping from around 3 to 3.1 ns after 300 s. While most C24-AgNCs showed fairly consistent decay times over the trajectory, 83 clusters (29%) undergo a significant change in the fluorescence decay time (determined to be a change of more than 20% of the average value) before photobleaching. The overall distribution of

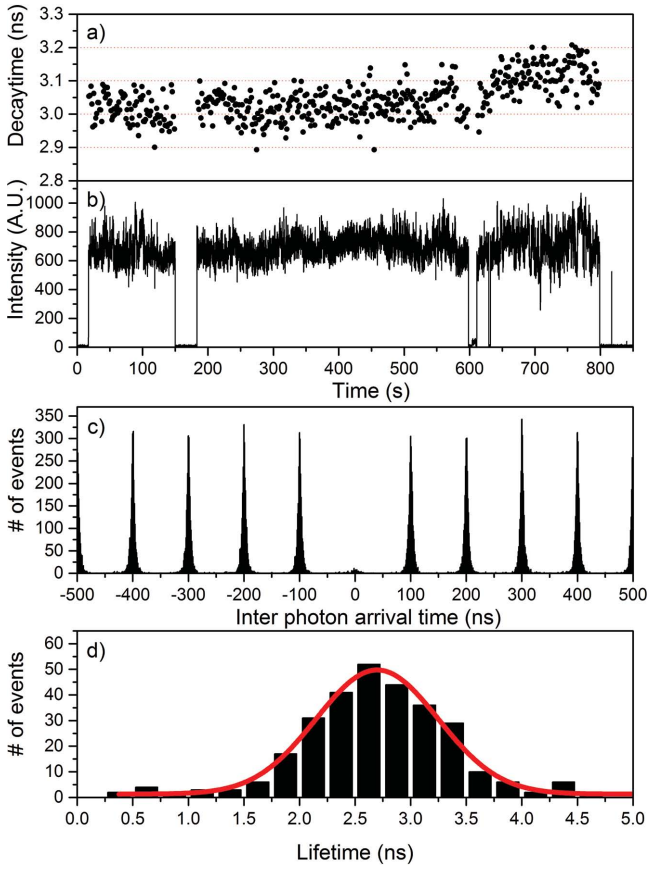

Figure 1. A typical fluorescence trace of a single C24-AgNC in PVA showing a) fluorescence decay time calculated every 10 000 photons, b) emitted photons over time in 10 ms bins, c) photon correlation plot of the whole trace (b) showing photon antibunching, and d) a histogram of average fluorescence decay times, fitted with a Gaussian function centered around 2.7 ns.

the average decay times of the 285 C24-AgNCs is broad and centered around 2.7 ns, slightly shorter than the dominant decay component of 3.09 ns found in the bulk experiments, but still similar to other reports.[4,6] The broad Gaussian-like distribution of the decay times suggests that the sample does not consist of several distinct species with well-defined decay times, but points to an inherent inhomogeneity of the polymer matrix embedded C24-AgNCs. The small difference in the decay time between the bulk sample and the isolated single molecules could be due to changes in the conformation of the DNA in the polymer film compared to in solution. The bias of single molecule spectroscopy towards bright and photostable molecules should also not be neglected, and differences to the bulk data may be due to the fact that dimmer clusters might not be measured at the single molecule level.

2.3. Single Molecule Measurements: Emission Spectra versus Decay Times

To investigate whether there is a link between fluorescence decay times and the emission spectra (suggesting several well defined classes of emitting species) both were measured simultaneously for all single C24-AgNC. The fluorescence signal was split and half of the photons were sent to a spectrograph with a charge-coupled device (CCD) camera. Spectra were measured with an integration time of 10 s, (**Figure 2**a). The spectra showed the distinct Gaussian shape associated with AgNC emission.[14,25,27,31] Each spectrum was fitted to a Gaussian function to determine the emission maximum. A histogram of the average emission maxima of all the single molecules is shown in Figure 2d along with the emission spectrum of the bulk sample. Examples of three distinct single C24-AgNC spectra versus the bulk solution spectra are shown in Figure S4 (Supporting Information) and clearly show that the single molecule emission spectra have a narrower full width at half maximum (FWHM) (≈40% narrower on average, as determined by analysis of 105 single AgNC spectra). This result is expected even at room temperature, although the spectra are not as narrow as those measured in cryogenic conditions.[27] The distribution of the average emission maxima looks to display a bimodal distribution with maxima centered around 660 and 690 nm. This could indicate the presence of two types of emitters. The distribution of single molecule spectra appears to be shifted to the blue compared to the bulk sample, with a maximum around 660 nm, rather than 700 nm for the bulk. However, this is most likely due to the different relative intensities of the different molecules. Molecules with a blueshifted spectrum are more common, but tend to be less bright. (see also **Figure 3**c,d). Again one cannot exclude the possibility that immobilization on the PVA alters the observed spectral characteristics slightly versus the solution case.

Besides constructing the individual distributions of the decay times and emission maxima, we correlated both to see if there is any trend. Figure 3a shows the average emission maxima plotted against the average fluorescence decay time of each AgNC bright enough to record emission spectra from. The distribution shows no specific correlation, meaning that the fluorescence decay time is distributed similarly over the emission wavelength range. If there are two distinct types of emitters

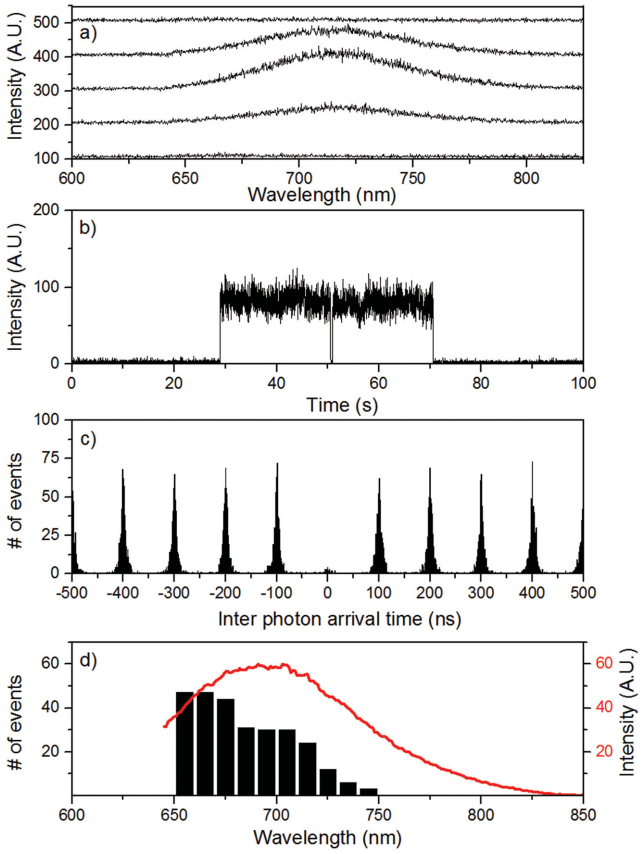

Figure 2. A typical fluorescence trace of a single C24-AgNC in PVA showing a) emission spectra collected every 10 s, b) emitted photons over time in 10 ms bins, c) photon correlation plot of the whole trace (b) showing photon antibunching, and d) a histogram of average emission maxima overlaid with the bulk emission spectrum (red).

as one might conclude from the histogram in Figure 2d, they seem to have a similar distribution of decay times. It could also be that this histogram does not represent fractions that were not bright enough to obtain an emission spectrum at the single molecule level. Additionally, there is no correlation between the total survival time (defined as the amount of time until photobleaching) and the spectral maxima (Figure 3b). A correlation does exist between the average emission intensity of the C24-AgNC and its spectral maximum, as shown in Figure 3c. C24-AgNCs with blueshifted emission tend to have lower average intensities. Separating the traces by intensity (Figure 3d) clearly shows the tendency for dim clusters to have blueshifted emission spectra, whereas brighter clusters have a much broader range of emission maxima. Molecules with intensities below 100 counts per 10 ms show a significant shift towards "blue" emission. The tendency is present, albeit less pronounced, in clusters with emission rates between 100 and 200 counts per 10 ms. For intensities above those values, the distribution becomes broader and more Gaussian with a maximum centered around 690 nm for the 200–300 counts per 10 ms case. The latter strengthens the previous idea that there might be two types of emitters. A dimmer one with emission maxima centered around 660 nm and a brighter one with a broader distribution of emission maxima centered around

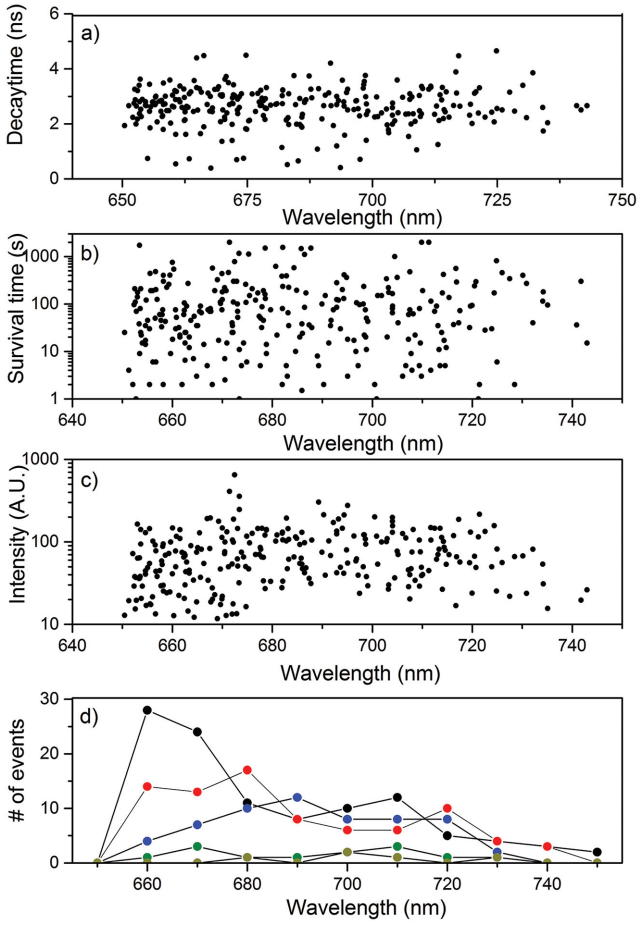

Figure 3. Plots depicting the relationship between the average emission maximum for each nanocluster versus a) fluorescence decay time, b) total survival time before photobleaching, and c) average emission intensity. A histogram of emission maxima at different emission intensities (d), from 0 to 100 (black), 100 to 200 (red), 200 to 300 (blue), 300 to 400 (green), and 400 to 500 (yellow) counts per 10 ms. Higher emission rates are not shown.

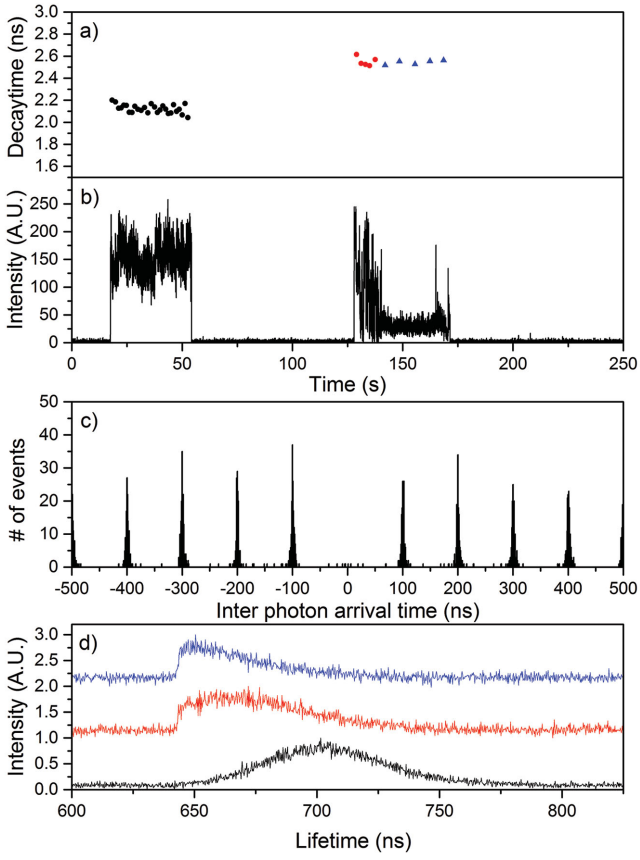

Figure 4. A fluorescence trace of a single C24-AgNC in PVA showing a) fluorescence lifetime calculated every 10 000 photons, color coded to correspond to the three spectral regions depicted in panel d), b) emitted photons over time in 10 ms bins, c) photon correlation plot of the trace showing photon antibunching, and d) three emission spectra measured from (approx.) 10–25 s (black), 65–70 s (red) and 70–88 s (blue). (The blue edge of the spectra is cut off by the dichroic mirror.)

690 nm. One possible reason for the lower intensity of the blueshifted emitters is that they could be less efficiently excited at 635 nm and a part of the emission spectrum is missing (see also Figure S4, Supporting Information).

Even within a single C24-AgNC measurement, fluctuations to both the decay time and emission maxima can occur, with little correlation to one another. **Figure 4** shows a single C24-AgNC intensity trajectory, with the fluorescence decay times and emission spectra, as a function of time. Large changes to both the decay time and emission spectra occur after the long "off" period between 25 and 60 s. The large blueshift of the spectrum (≈40 nm) is accompanied by an increase in the fluorescence decay time from 2.2 to 2.6 ns. At 70 s, a large decrease in the intensity of the C24-AgNC is accompanied by a further blueshift in the emission spectrum; however, the fluorescence decay time shows very little change. Lack of change in the fluorescence decay time suggests that the drop in intensity is most likely not due to quenching. Figure 4 and the extra examples in Figures S5–S7 (Supporting Information) show changes in the emission spectrum and decay time over time, suggesting that changes could be linked to, for example, a change in the conformation of the DNA or the emissive AgNC itself. These changes were observed for C24-AgNC that displayed single emitter behavior (as seen by the photon antibunching behavior), ruling out the possibility that multiple independent emitters were present and caused the change in behavior.

Of the 285 molecules measured, 78 (27%) showed significant changes in the emission spectrum. Forty-two percent of the molecules exhibiting spectral shifting show only blueshifts, 25% show distinct redshifts, and the remaining 34% show both red and blueshifts within a single trace. Examples of some of these traces can be found in Figures S5–S7 (Supporting Information). Similar trends can be seen in the fluorescent decay times. As mentioned before, these changes do not necessarily correlate with one another, only 41 (14%) of the molecules showed changes in both fluorescence decay time (as defined as more than 20% change) and emission spectra. The latter also shows that a change in the emission spectrum is not necessarily accompanied by a change in the decay time. An example of this can be seen in Figure 4 where from 60 to 95 s we see a

blueshift (Figure 4d, red to blue spectrum) of the spectrum but the decay time stays the same.

2.4. Single Molecule Measurements: Antibunching

Abrupt changes to the behavior of C24-AgNCs could be explained by the fact that more than one cluster is within the confocal volume and upon photobleaching of one emitter; the other's characteristics become more apparent. In order to exclude this possibility, antibunching measurements were performed on all the measured C24-AgNCs, and the results show that the overwhelming majority behaved as single emitters. An example of a single C24-AgNC fluorescence intensity trajectory with the antibunching histogram is given in **Figure 5**a,b. Photon correlation plots are also shown for all the other examples in Figures 1c, 2c, and 4c, and Figures S5–S7 (Supporting Information). A histogram of N_C/N_1 values (Figure 5c), where N_C represents the photons in the central peak at 0 ns delay and N_I the photons in the lateral peaks, shows that most clusters had a ratio of less than 0.2. Any measurements with a ratio higher than 0.2 (11 out of 300) were disregarded from all analysis in this paper. Therefore, the results presented in this paper show that the C24-AgNCs that we studied behaved as single emitters under the given excitation conditions.

The clear photon antibunching and lack of correlation between changes in the fluorescent decay times and spectral maxima suggest that the varied behavior of the individual clusters is due to a response to changes in the AgNC or its local environment. Small adjustments in the conformation of the DNA[39] may contribute to changes in decay time or emission maximum. It is tempting to attribute any changes over time to photooxidation or a reversible redox reaction. However, as both red and blueshifting is observed, it is unlikely that a single process is responsible. Additionally, oxidation or even partial oxidation of a silver cluster has been shown to have a very large effect on the emission spectrum, usually a clear blueshift outside the region where we can still excite the C24-AgNCs[40,41] The changes observed in this case are generally below 100 nm. Fluorophores can undergo small changes to their conformation, even when suspended in a polymer matrix,[42,43] which can lead to changes in their inherent fluorescent properties. Although it has been shown that DNA conformation is relatively stable in PVA films,[44] small fluctuations are likely given the large void size and inhomogeneous nature of PVA films.[45] From the perspective of a silver nanocluster, the conformation of the scaffold has a large effect on its behavior,[46] as the scaffold dictates the angle of the silver atoms with relation to one another.[47] Changes in the proximity of silver ions can also affect the highest occupied molecular orbital - lowest unoccupied molecular orbital (HOMO–LUMO) gap and change the photophysical properties.[24]

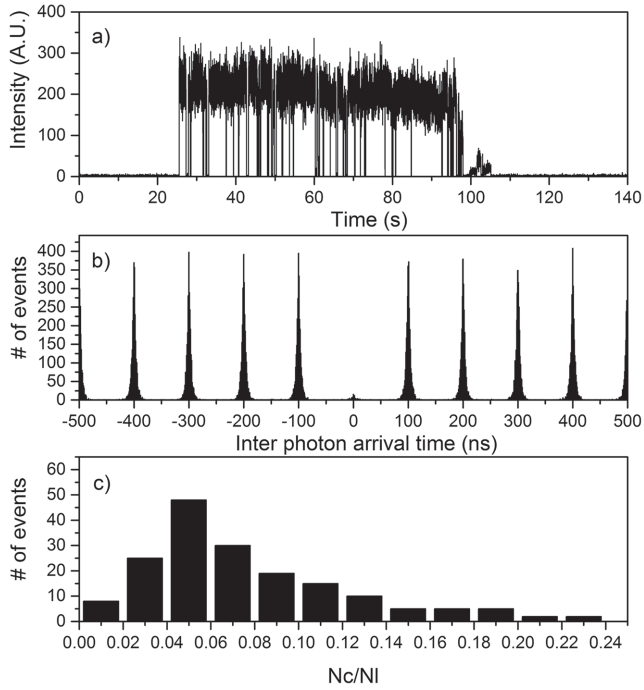

Figure 5. A fluorescence trace of a single C24-AgNCs in PVA showing a) emitted photons over time in 10 ms bins, b) photon correlation plot of the trace showing photon antibunching, and c) a histogram of N_C/N_I ratios.

2.5. Single Molecule Measurements: Blinking

Blinking in fluorescence intensity trajectories of AgNCs in DNA in the microsecond time range have been previously attributed to electron or charge transfer to the surrounding DNA.[11,47,48] This blinking process can be studied at the single molecule level by performing an autocorrelation analysis on the fluorescence intensity trajectory.[49] Second order autocorrelation functions (ACF) were generated from the fluorescence traces and most C24-AgNCs showed autocorrelation curves that could be fitted with a two exponential model (The second, longer time component usually has a very small amplitude and was therefore not analyzed in detail). The biexponential ACF generated from the trajectory in **Figure 6**b over the time range 35–45 s (where longer "off" periods on the seconds time scale are absent) is shown in Figure 6a. For the fast correlation component, off times were calculated from the autocorrelation fit, using a three state model and a histogram of calculated off times is shown in Figure 6d.[49] The histogram can be fitted with a Gaussian distribution, centered around 32 µs, which matches well with previous reports of off times on AgNCs.[6] The histogram does feature a long tail, with off times in the order of hundreds of microseconds. It has been shown previously that the value of this microsecond off time can be dependent on the excitation power and can virtually disappear when an appropriate additional wavelength is used.[32] In addition to this analysis of the short blinking, one can observe also the presence of very long off times in the second to tens of seconds time scale (see examples in the fluorescence time trajectory of Figures 1,4, and 6, and Figures S5–S7, Supporting Information). It is unclear what causes these very long off states. The low number of events makes it difficult to extract an accurate time constant or to verify whether they follow an exponential or power-law distribution.[50]

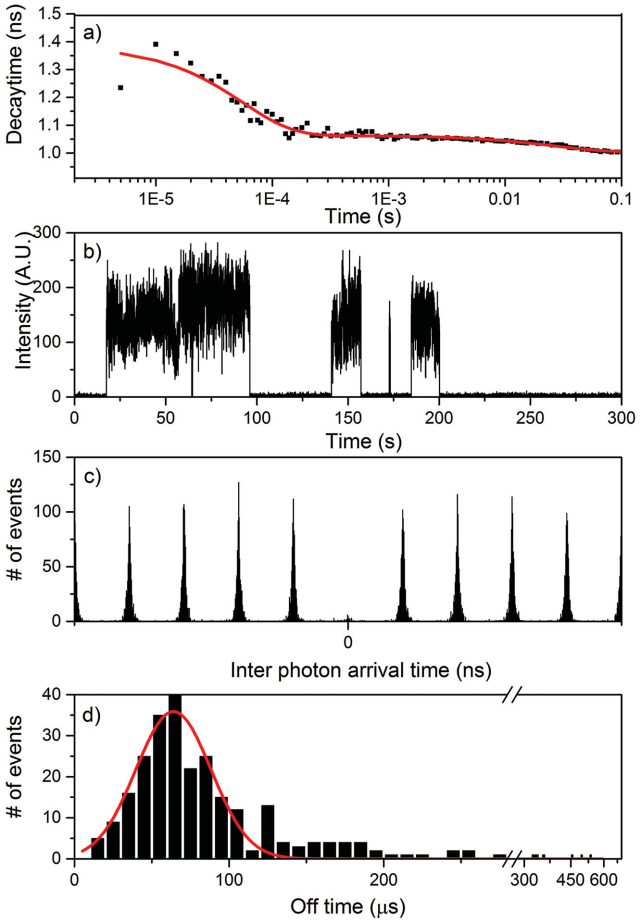

Figure 6. A fluorescence trace of a single C24-AgNCs in PVA showing a) autocorrelation decay (black), fitted to two exponentials (red), b) emitted photons over time in 10 ms bins, c) correlation plot of the trace showing photon antibunching, and d) histogram of calculated "off" times for the faster component in the autocorrelation decay (black), fitted with a Gaussian function (red).

3. Conclusions

Single molecule spectroscopy was performed on a sample of silver nanoclusters stabilized in ssDNA containing 24 cytosines. Polycytosines are known to stabilize a whole range of emissive species throughout the visible range. Here we employed single molecule spectroscopy to probe a subsection of near-infrared emitters in order to characterize the photophysical heterogeneity by measuring decay times, emission spectra, and antibunching simultaneously. Our findings indicate that in the spectral range that we probe upon 635 nm excitation, the sample exhibited a broad distribution of photophysical properties for two types of emissive species. No clear correlation between decay time and emission maximum was observed, indicating that in the spectral range we probed, we do not have spectrally well-defined emitters with narrow emission maxima distributions with specific associated decay times. Additionally, the single molecule measurements revealed that some of the C24-AgNCs can change their spectral properties such as emission maximum and decay time during the measurement without any obvious trends. Photon antibunching measurements were performed on all C24-AgNCs to verify that the changes in photophysical properties were not due to the presence of multiple independent emitters. Therefore, we believe that the observed changes to C24-AgNCs show the presence of an inherent flexibility to alter its emissive properties. The exact mechanism that could explain these changes is not addressed, but changes in the AgNCs geometry, local environment (e.g. proximity of silver ions) or changes in the DNA conformation could be likely candidates. Although large changes in emission maxima are most likely related to, for example, differences in the number of atoms and the charge of the silver nanoclusters, the smaller, more gradual changes observed in the bulk emission spectra upon changing the exaction wavelength could be attributed to the aforementioned explanation.

4. Experimental Section

Synthesis: Silver nanoclusters were synthesized according the procedure published by Petty et al.[51] Silver nitrate (99.9999%, Sigma-Aldrich) and sodium borohydride (99.99%, Sigma-Aldrich) were used as precursor and reagent, respectively. For stabilizing the AgNCs, single stranded oligonucleotide dC24 (Reverse Phase-Cartridge-Gold purification, Eurogentec) was used as scaffold. All the reactants were dissolved in ultrapure Milli-Q deionized water (referred to as MQ in the text) without any further purification. The DNA sample was thawed and then dissolved in a volume of MQ to obtain a final concentration of 2×10^{-3} M. A 2×10^{-3} M $AgNO_3$ solution was prepared and a volume equal to 12 times the volume of DNA was added to the DNA solution. The sample was shaken 2 min to allow a homogeneous interaction of Ag^+ and C24 sequence. $NaBH_4$ salt was dissolved in MQ to a concentration of 2×10^{-3} M and a volume equal to 12 times the volume of DNA sample was added and The final solution was agitated for 2 min. Globally, the following proportion of moles between the different components of the synthesis route was respected: (1:12:12) = (DNA:$AgNO_3$:$NaBH_4$).

Ensemble Measurements: Steady-state luminescence measurements of bulk sample were acquired using a Fluorolog-2 (Spex, F112AI) fluorometer. The emission spectra were collected with an excitation wavelength of 635 nm. The average emission spectrum maxima were calculated by averaging the first 20 spectra.

TC-SPC experiments were performed on a Fluo Time 300 (Picoquant) using a pulsed 635 nm laser (Picoquant, LDH-P-635).

Single Molecule Measurements: Single molecule measurements were made on a homebuilt confocal microscope described in detail by Liao et al.[52] Briefly, a sample of silver nanoclusters was diluted in a saturated solution of PVA (Aldrich) in MQ water. This solution was spincast onto a clean glass coverslip (Menzel 22 mm × 22 mm × 170 μm). The dilution was performed until a limited number of spots appeared in a 10 × 10 μm image, (see Figure S1, Supporting Information). The excitation source was a 635 nm pulsed laser diode (Picoquant, 100 MHz and 108 W cm^{-2} on the sample for all experiments), focused through an Olympus IX71 microscope by the oil immersion objective lens (Olympus UPLFLN 100×). Scatter from the excitation source was removed using a longpass filter (Semrock LP02-633RU-25). The fluorescence signal was split by a 50–50 beamsplitter (Thorlabs), with half collected by two avalanche photodiodes (APDs, Perkin-Elmer CD3226) in a Hanbury Brown-Twiss arrangement,[53] the other half by a spectrograph and cooled CCD camera (Princeton Instruments SPEC-10:100B/LN_eXcelon CCD camera, SP 2356 spectrometer). The signals from the APDs were fed into a SPC-830 card (Becker & Hickl) with one APD delayed by a DG535 delay generator (Stanford Research Systems).

Supporting Information

Supporting Information is available from the Wiley Online Library or from the author.

Acknowledgements

T.V. gratefully acknowledges financial support from the "Center for Synthetic Biology" at Copenhagen University funded by the UNIK research initiative of the Danish Ministry of Science, Technology and Innovation (Grant 09-065274); bioSYNergy, University of Copenhagen's Excellence Programme for Interdisciplinary Research; the Carlsberg Foundation, the Villum Foundation (Project No. VKR023115) and the Danish Council of Independent Research (Project No. DFF-1323-00352). We would also like to thank Bo Wegge Laursen and Thomas Just Sørensen for use of equipment and Christian Brueffer for assistance with data analysis.
Note: Further information on the emission spectrum measurements was added to the Ensemble Measurements part of the Experimental Section on August 18, 2015, after initial publication online.

Received: January 21, 2015
Revised: March 17, 2015
Published online: April 17, 2015

[1] H. Xu, K. S. Suslick, *Adv. Mater.* **2010**, *22*, 1078.
[2] J. Zheng, P. R. Nicovich, R. M. Dickson, *Annu. Rev. Phys. Chem.* **2007**, *58*, 409.
[3] I. Díez, R. H. A. Ras, *Nanoscale* **2011**, *3*, 1963.
[4] S. Choi, R. M. Dickson, J. Yu, *Chem. Soc. Rev.* **2012**, *41*, 1867.
[5] C. I. Richards, S. Choi, J. Hsiang, Y. Antoku, T. Vosch, A. Bongiorno, Y. Tzeng, R. M. Dickson, *J. Am. Chem. Soc* **2008**, *130*, 5038.
[6] T. Vosch, Y. Antoku, J.-C. Hsiang, C. I. Richards, J. I. Gonzalez, R. M. Dickson, *Proc. Natl. Acad. Sci. USA* **2007**, *104*, 12616.
[7] D. Schultz, E. G. Gwinn, *Chem. Commun.* **2012**, *48*, 5748.
[8] J. T. Petty, C. Fan, S. P. Story, B. Sengupta, A. S. Iyer, Z. Prudowsky, R. M. Dickson, *J. Phys. Chem. Letts.* **2010**, *1*, 2524.
[9] N. Makarava, A. Parfenov, I. V. Baskakov, *Biophys. J.* **2005**, *89*, 572.
[10] T. H. Lee, J. I. Gonzalez, J. Zheng, R. M. Dickson, *Acc. Chem. Res.* **2005**, *38*, 534.
[11] S. A. Patel, M. Cozzuol, J. M. Hales, C. I. Richards, M. Sartin, J. Hsiang, T. Vosch, J. W. Perry, R. M. Dickson, *J. Phys. Chem. C* **2009**, *113*, 20264.
[12] D. D. Evanoff, G. Chumanov, *ChemPhysChem* **2005**, *6*, 1221.
[13] M. Mukherjee, S. K. Saha, D. Chakravorty, *Appl. Phys. Lett.* **1993**, *63*, 42.
[14] J. Zheng, R. M. Dickson, *J. Am. Chem. Soc.* **2002**, *124*, 13982.
[15] J. Yu, S. A. Patel, R. M. Dickson, *Angew. Chem. Int. Ed.* **2007**, *46*, 2028.
[16] J. Xie, Y. Zheng, J. Y. Ying, *J. Am. Chem. Soc.* **2009**, *131*, 888.
[17] E. G. Gwinn, P. O'Neill, a. J. Guerrero, D. Bouwmeester, D. K. Fygenson, *Adv. Mater.* **2008**, *20*, 279.
[18] C. M. Ritchie, K. R. Johnsen, J. R. Kiser, Y. Antoku, R. M. Dickson, J. T. Petty, *J. Phys. Chem. C* **2007**, *111*, 175.
[19] S. M. Copp, P. Bogdanov, M. Debord, A. Singh, E. G. Gwinn, *Adv. Mater.* **2014**, *26*, 5839.
[20] S. Walczak, K. Morishita, M. Ahmed, J. Liu, *Nanotechnology* **2014**, *25*, 155501.
[21] Y. Antoku, J. Hotta, H. Mizuno, R. M. Dickson, J. Hofkens, T. Vosch, *Photochem. Photobiol. Sci.* **2010**, *9*, 716.
[22] J. Yu, S. Choi, C. I. Richards, Y. Antoku, R. M. Dickson, *Photochem. Photobiol.* **2008**, *84*, 1435.
[23] J. Sharma, H. Yeh, H. Yoo, J. H. Werner, J. S. Martinez, *Chem. Commun.* **2010**, *46*, 3280.
[24] S. M. Copp, D. Schultz, S. Swasey, J. Pavlovich, M. Debord, A. Chiu, K. Olsson, E. G. Gwinn, *J. Phys. Chem. Lett.* **2014**, *5*, 959.
[25] D. Schultz, K. Gardner, S. S. R. Oemrawsingh, N. Markešević, K. Olsson, M. Debord, D. Bouwmeester, E. G. Gwinn, *Adv. Mater.* **2013**, *25*, 2797.
[26] P. R. O'Neill, L. R. Velazquez, D. G. Dunn, E. G. Gwinn, D. K. Fygenson, *J. Phys. Chem. C* **2009**, *113*, 4229.
[27] S. S. R. Oemrawsingh, N. Markeševi , E. G. Gwinn, E. R. Eliel, D. Bouwmeester, *J. Phys. Chem. C* **2012**, *116*, 25568.
[28] N. Markešević, S. S. R. Oemrawsingh, D. Schultz, E. G. Gwinn, D. Bouwmeester, *Adv. Opt. Mater.* **2014**, *2*, 765.
[29] L. A. Peyser, A. E. Vinson, A. P. Bartko, R. M. Dickson, *Science* **2001**, *291*, 103.
[30] P. Kumar, A. Mehta, M. D. Dadmun, J. Zheng, L. Peyser, A. P. Bartko, R. M. Dickson, T. Thundat, B. G. Sumpter, D. W. Noid, M. D. Barnes, *J. Phys. Chem. B* **2003**, *107*, 6252.
[31] T. Lee, R. M. Dickson, *Proc. Natl. Acad. Sci. USA* **2003**, *100*, 3043.
[32] C. I. Richards, J. Hsiang, D. Senapati, S. Patel, J. Yu, T. Vosch, R. M. Dickson, *J. Am. Chem. Soc.* **2009**, *131*, 4619.
[33] P. R. O'Neill, K. Young, D. Schiffels, D. K. Fygenson, *Nano Lett.* **2012**, *12*, 5464.
[34] S. Park, S. Choi, J. Yu, *Nanoscale Res. Lett.* **2014**, *9*, 129.
[35] L. Maretti, P. S. Billone, Y. Liu, J. C. Scaiano, *J. Am. Chem. Soc.* **2009**, *131*, 13972.
[36] B. Karthikeyan, *J. Appl. Phys.* **2008**, *103*, 114313.
[37] W. E. Moerner, *J. Phys. Chem. B* **2002**, *106*, 910.
[38] K. Morishita, J. L. MacLean, B. Liu, H. Jiang, J. Liu, *Nanoscale* **2013**, *5*, 2840.
[39] T. Driehorst, P. O'Neill, P. M. Goodwin, S. Pennathur, D. K. Fygenson, *Langmuir* **2011**, *27*, 8923.
[40] S. Choi, S. Park, K. Lee, J. Yu, *Chem. Commun.* **2013**, *49*, 10908.
[41] Y. Antoku, *Ph.D. Thesis*, Georgia Tech, Atlanta, **2007**.
[42] J. M. Lupton, *Adv. Mater.* **2010**, *22*, 1689.
[43] J. Hofkens, T. Vosch, M. Maus, F. Köhn, M. Cotlet, T. Weil, A. Herrmann, K. Muellen, F. C. De Schryver, *Chem. Phys. Lett.* **2001**, *333*, 255.
[44] P. Hanczyc, B. Norden, B. Åkerman, *J. Phys. Chem. B* **2011**, *115*, 12192.
[45] P. Hanczyc, B. Åkerman, B. Nordén, *Langmuir* **2012**, *28*, 6662.
[46] I. Díez, R. H. a Ras, M. I. Kanyuk, A. P. Demchenko, *Phys. Chem. Chem. Phys.* **2013**, *15*, 979.
[47] R. R. Ramazanov, A. I. Kononov, *J. Phys. Chem. C* **2013**, *117*, 18681.
[48] L. Zhang, J. Zhu, S. Guo, T. Li, J. Li, E. Wang, *J. Am. Chem. Soc.* **2013**, *135*, 2403.
[49] W.-T. Yip, D. Hu, J. Yu, D. A. Vanden Bout, P. F. Barbara, *J. Phys. Chem. A* **1998**, *102*, 7564.
[50] F. Cichos, M. Orrit, *Curr. Opin. Colloid Interface Sci* **2007**, *12*, 272.
[51] J. T. Petty, J. Zheng, N. V Hud, R. M. Dickson, *J. Am. Chem. Soc.* **2004**, *126*, 5207.
[52] Z. Liao, E. N. Hooley, L. Chen, S. Stappert, K. Müllen, T. Vosch, *J. Am. Chem. Soc.* **2013**, *135*, 19180.
[53] R. Hanbury-Brown, R. Q. Twiss, *Nature* **1956**, *177*, 27.